Available online at www.sciencedirect.com
ScienceDirect
Journal of Power Sources 158 (2006) 1324–1332
JOURNAL OF POWER SOURCES
www.elsevier.com/locate/jpowsour

Development of an equivalent circuit model of a fuel cell to evaluate the effects of inverter ripple current

Woojin Choi [a,*], Jo.W. Howze [b,1], Prasad Enjeti [b,1]

[a] *Power Electronics & Renewable Energy Conversion Laboratory, Department of Electrical Engineering, Soongsil University, 1-1 Sangdo-dong, Dongjak-gu, Seoul 156-743, Republic of Korea*

[b] *Power Electronics & Fuel Cell Power-Conditioning Laboratory, Department of Electrical Engineering, Texas A&M University College Station, TX 77843-3128, USA*

Received 5 September 2005; received in revised form 10 October 2005; accepted 11 October 2005
Available online 28 November 2005

Abstract

In this paper, an impedance model of the proton exchange membrane fuel cell stack (PEMFCS) is proposed. The proposed study employs an equivalent circuit of the PEMFCS derived by the frequency response analysis (FRA) technique. An equivalent circuit for the fuel cell stack is developed to evaluate the effects of ripple currents generated by the power-conditioning unit. The calculated results are then verified by means of experiments on two commercially available fuel cells: Avista Labs SR-12 (500 W) and Ballard Nexa (1.2 kW) PEMFC system. The relationship between ripple current and fuel cell performance, such as power loss and fuel consumption is investigated. Experimental results show that the ripple current can contribute up to a 10% reduction in the available output power.

Keywords: Fuel cell; Modeling; Ripple current; Power reduction; Frequency response analysis technique; Equivalent circuit

1. Introduction

Fuel cells are expected to play an important role in the power generation field by virtue of their inherently clean, efficient and reliable service. Their use is spreading widely and promising applications include portable power, transportation, residential power and distributed power for utilities. Unlike conventional power sources, a fuel cell system can be highly efficient over the whole load range with little variation, scaled to a variety of sizes without performance deterioration and can be perfectly environmentally friendly. However, for further deployment, fuel cells are required to become more competitive in terms of cost and reliability.

Among the various types of fuel cells, the proton exchange membrane (PEM) fuel cell is drawing more attention due to its low operating temperature, ease of start-up and shut-down and compactness. The PEM fuel cell is providing reliable power at steady-states, however, it is not able to respond promptly to a load step change due to the delay time for the fuel flow rate to adjust. Since the fuel cell is an electrochemical energy conversion device that converts fuel into electricity, its dynamic behavior depends both on chemical and thermodynamic processes. Thus, in designing a fuel cell power system, it is required for the design engineer to understand the unique characteristics of the fuel cell to implement the best system in terms of efficiency and cost.

Various attempts have been made to model the proton exchange membrane fuel cell stack (PEMFCS). Almost all-recent endeavors in modeling [1–4], have neglected the effects of the inverter load due to reasons of simplicity. Several modeling methods have been suggested in the literature [1–5]. However, these modeling methods require fuel cell design parameters, which are not easy to obtain due to the proprietary nature of the technology. Furthermore, most of the models include complex chemical equations, which are not easy to solve and are not suitable for observing the electrical phenomena occurring when the fuel cell interacts with its power conditioning unit (PCU).

Since the fuel cell produces DC electricity, a power conditioning stage is essential to produce commercial AC power (120/240 V, 60 Hz). A typical fuel cell PCU employs switch-

* Corresponding author. Tel.: +82 10 2701 3823; fax: +82 2 817 7961.
E-mail addresses: cwj777@hanmail.net (W. Choi), enjeti@ee.tamu.edu (P. Enjeti).
[1] Tel: +1 979 845 7466.

0378-7753/$ – see front matter © 2005 Elsevier B.V. All rights reserved.
doi:10.1016/j.jpowsour.2005.10.038

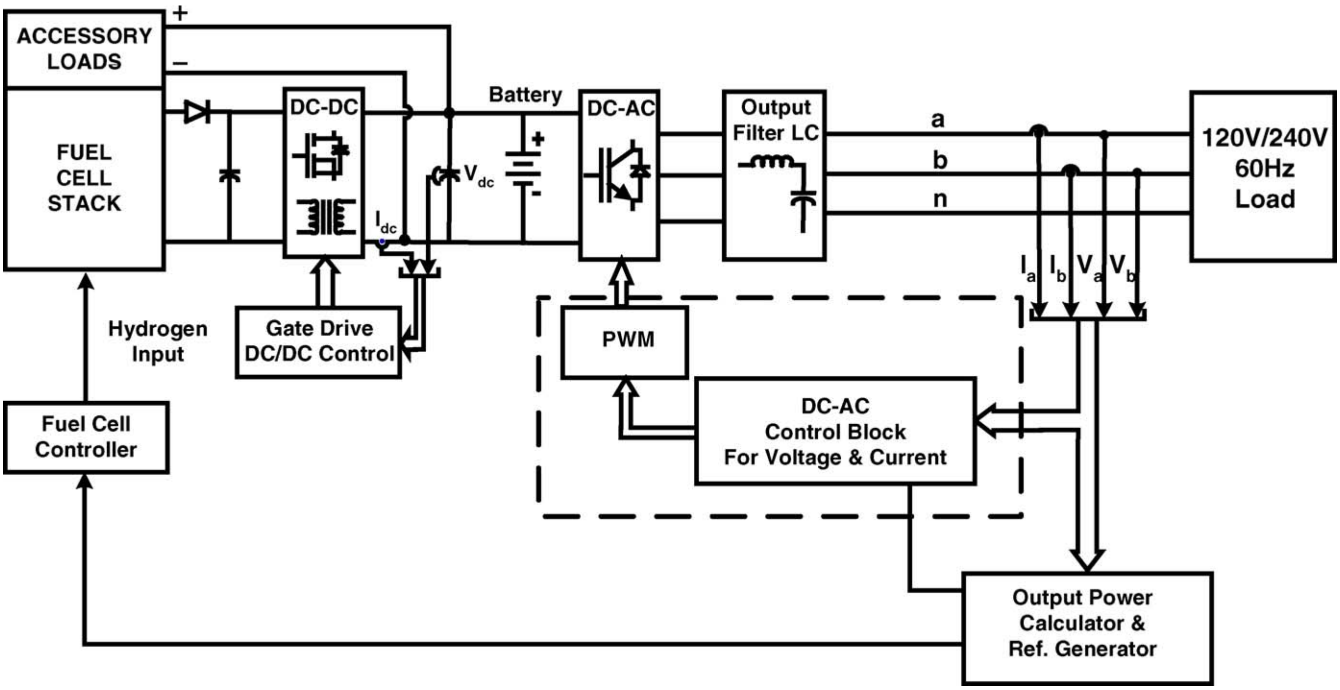

Fig. 1. Block diagram of a fuel cell power generation unit for supplying 120/240 V, 60 Hz load.

mode DC–DC and DC–AC converters (Fig. 1). Important variables for the design of the PCU are: (a) variation of fuel cell terminal voltage from no-load to full-load; (b) the amount of ripple current the fuel cell can tolerate. A large variation in fuel cell terminal voltage from no-load to full-load, results in larger volt-amp rating of the PCU. Also, for fuel cells powering single-phase loads (60 Hz), the ripple current is twice the output frequency, i.e. 120 Hz. The effect of the ripple current on the performance of a fuel cell stack has not been investigated thoroughly and so far remains uncertain [5].

Development of an equivalent circuit for a fuel cell by conducting a series of tests, to predict the electrical performance – including voltage regulation, rating of the PCU, dynamic behavior and the effects of inverter ripple current – is essential. A clear understanding of various factors including additional losses (if any) due to ripple current can contribute to better designs in the next generation fuel cell power systems.

In this paper, test results from two commercially available (Avista Lab SR-12 and Ballard Nexa) PEM fuel cells are fully analyzed. The proposed study employs an equivalent circuit of the PEM stack derived from the frequency response analysis (FRA) technique. The test results are then expressed in per-unit quantities to facilitate easy comparisons. The relationship between ripple current and fuel cell stack performance, such as power loss and fuel consumption is investigated. Experimental results indicate that ripple current can contribute up to 10%

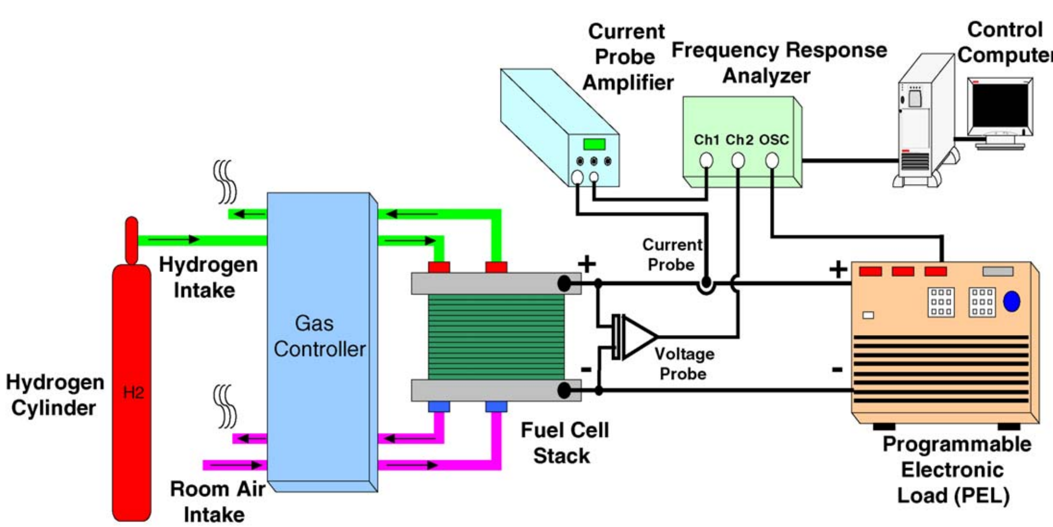

Fig. 2. Frequency response analysis technique: experimental setup for the fuel cell stack.

reduction in the available output power. This paper provides a detailed evaluation of these aspects, and includes a discussion of the frequency dependency of the fuel cell equivalent circuit parameters.

2. Modeling of the fuel cell stack with frequency response analysis (FRA) technique

Fig. 2 shows the experimental setup to evaluate the performance of the fuel cell stack under test. The setup consists of: proton exchange membrane fuel cell stack (PEMFCS), programmable electronic load (PEL, Chroma 63201), frequency response analyzer (FRA, Venable Model 260), current/voltage probes (Tektronix AM503B Current Amplifier and A6303 Current Probe, Tektronix P5205 Differential Voltage Probe) and a computer with the analysis software. The test setup was used to perform both DC and AC tests described in the next sections. In the experiments, hydrogen (>99.99% at 5 psig) and air are supplied to each PEMFCS and no humidification process was required for fuel and oxidant. It usually takes several minutes for a PEM fuel cell to become stable because the membrane needs to be humidified for optimum performance. Thus, before the test, both PEMFCSs were started after a short period of warm-up and then run for an hour at the full-load to ensure a thermally stable operation. Once the stack reached a stable operating condition, all the control variables, such as reactant flow rate and temperature were regulated by the system controller. The hydrogen flow rate in each experiment wass measured by the Mass Flow Controller (M100B, MKS Instruments). It should be noticed that the entire test was performed repeatedly and consistent data have been obtained.

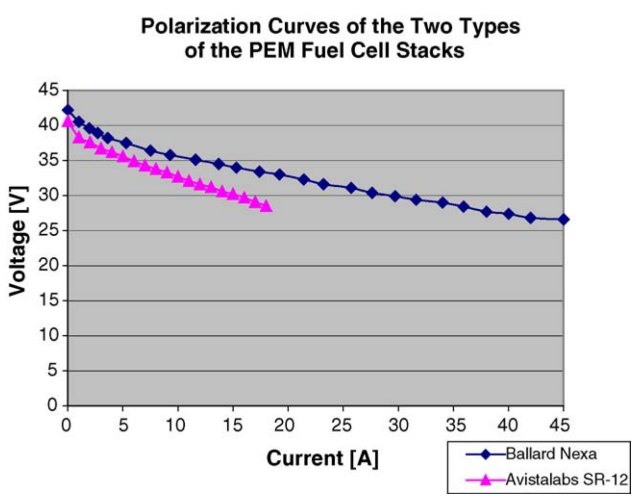

Fig. 3. Polarization (*V*–*I*) curves of the two types of the PEM fuel cell stacks.

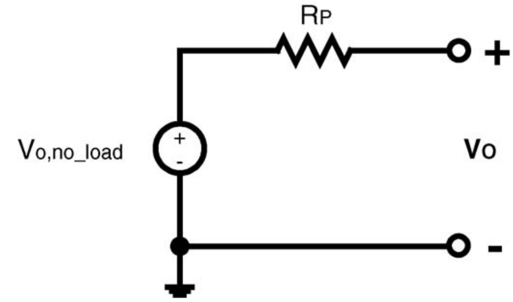

Fig. 4. DC equivalent circuit of the fuel cell stack.

2.1. DC equivalent circuit

In this test, the fuel cell is supplied with hydrogen and the electrical load (DC) was varied from zero to full-load (rated). The fuel cell terminal voltage variation is plotted for various output current settings in Fig. 3. The *V*–*I* curve (or polarization curve) is somewhat non-linear for lower values of current and exhibits a nearly linear behavior for load currents >25%. If we neglect the initial non-linearity, a simplified electrical equivalent circuit for the fuel cell can be obtained by calculating the slope of the *V*–*I* curve (Fig. 3). Fig. 4 shows the equivalent circuit with a resistance in series with the DC voltage source.

To facilitate the comparison between different ratings of fuel cells with different output voltage and current ratings, a per-unit system is developed. Table 1 shows the base definitions of per-unit quantities for the fuel cells under test. The resistance R_P

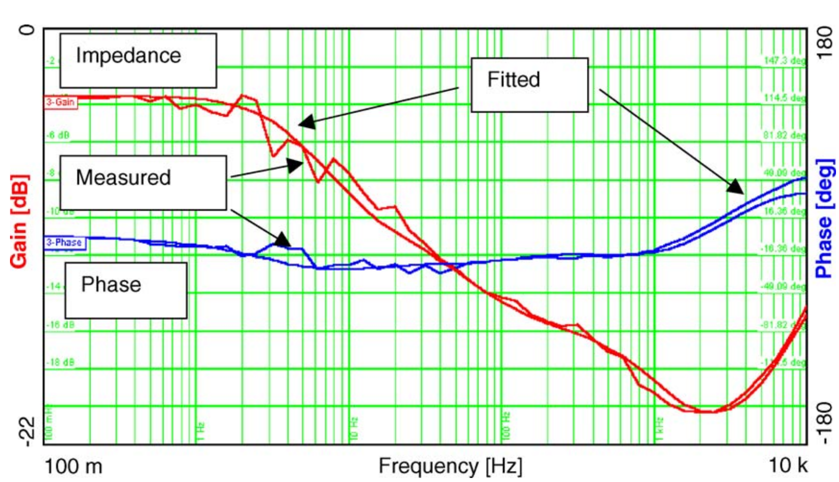

Fig. 5. Measured impedance spectrum of the PEMFCS and its curve fitting results.

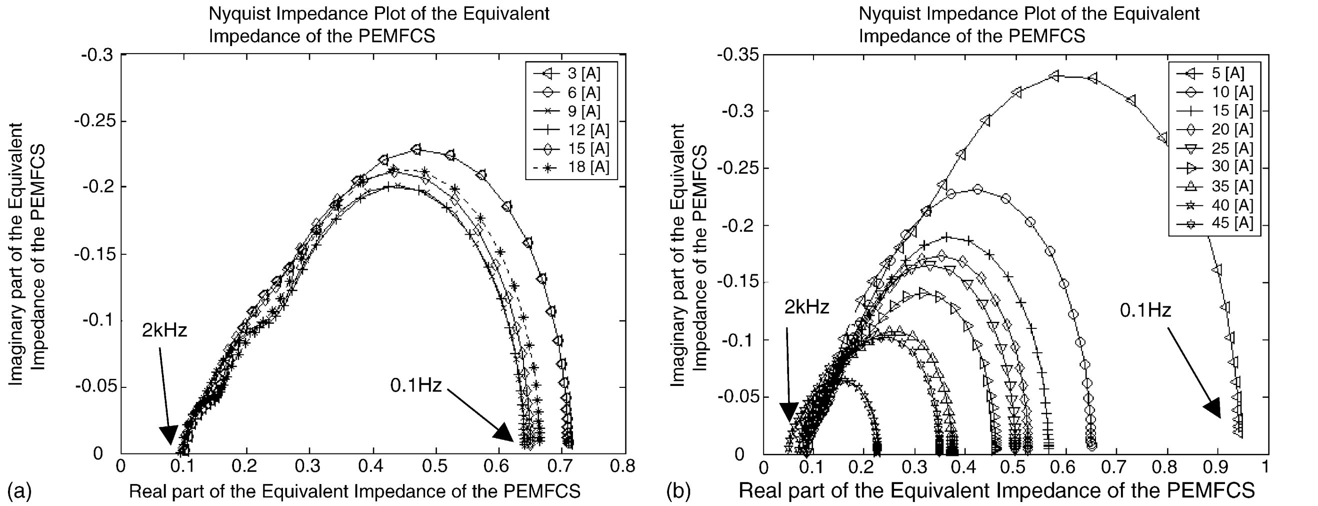

Fig. 6. (a) Nyquist impedance plot of the Avista Labs SR-12 PEMFCS at the different operating points and (b) Nyquist impedance plot of the Ballard Nexa PEMFCS at the different operating points.

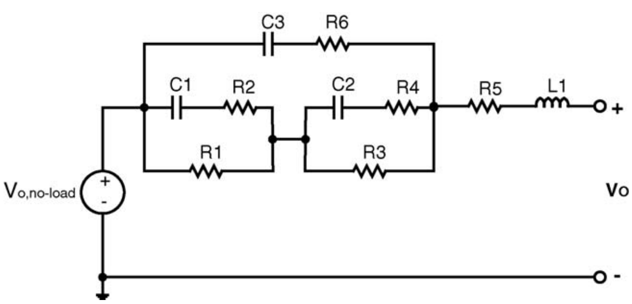

Fig. 7. Equivalent circuit of the PEMFCS at a certain operating point.

Table 1
Base definitions of per unit quantities for the PEMFCs under test

Fuel cell type	$V_{\text{o, no-load}}$ [V]	V_{base} [V]	I_{base} [A]	P_{base} [W]	Z_{base} [Ω]
SR-12	40.6	28.9	17.3	500	1.67
Nexa	42.2	26.6	45	1200	0.59

Where $V_{\text{o, no-load}}$: fuel cell stack voltage at no-load; V_{base}: fuel cell stack voltage at full-load; I_{base}: rated (full-load) current (rms); P_{base}: rated output power; $Z_{\text{base}} = V_{\text{base}}/I_{\text{base}}$: base impedance.

shown in fuel cell equivalent circuit (DC) can be calculated as:

$$R_{\text{P}} = \frac{V_{\text{o, no-load}} - V_{\text{o, full-load}}}{I_{\text{full-load}}} \tag{1}$$

This can be represented in per-unit as:

$$R_{\text{P, per-unit}} = \frac{R_{\text{P}}}{Z_{\text{base}}} \tag{2}$$

Since the fuel cell *V–I* curve shows a wide variation in output voltage (V_{o}) from no-load to full-load, a voltage regulation factor (VRF) is defined:

$$\text{VRF} = \frac{V_{\text{o, no-load}} - V_{\text{o, full-load}}}{V_{\text{o, full-load}}} \tag{3}$$

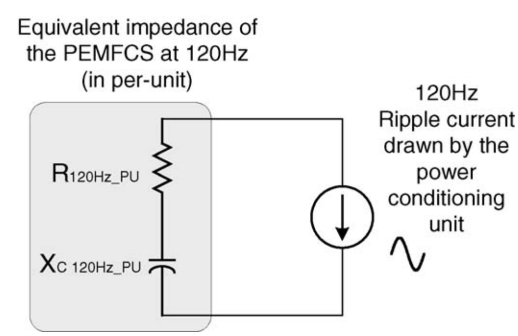

Fig. 9. AC equivalent circuit of the fuel cell stack at 120 Hz.

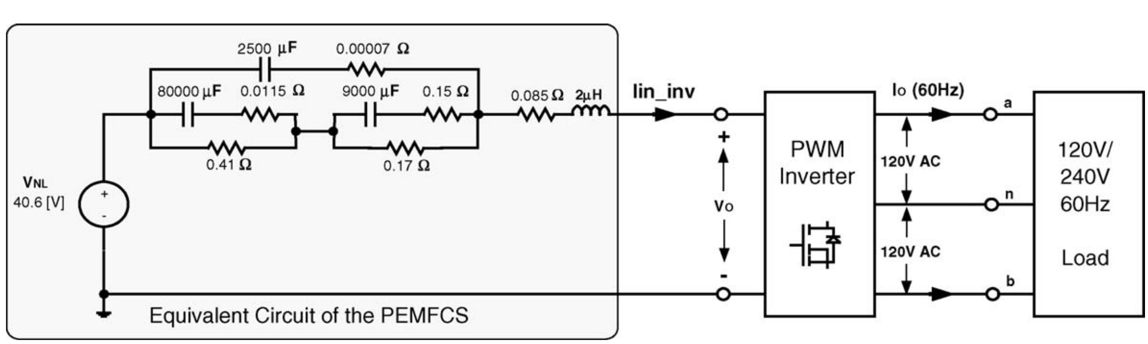

Fig. 8. Interconnection of the fuel cell equivalent circuit with the power conditioning unit to facilitate the evaluation of the effect of ripple current.

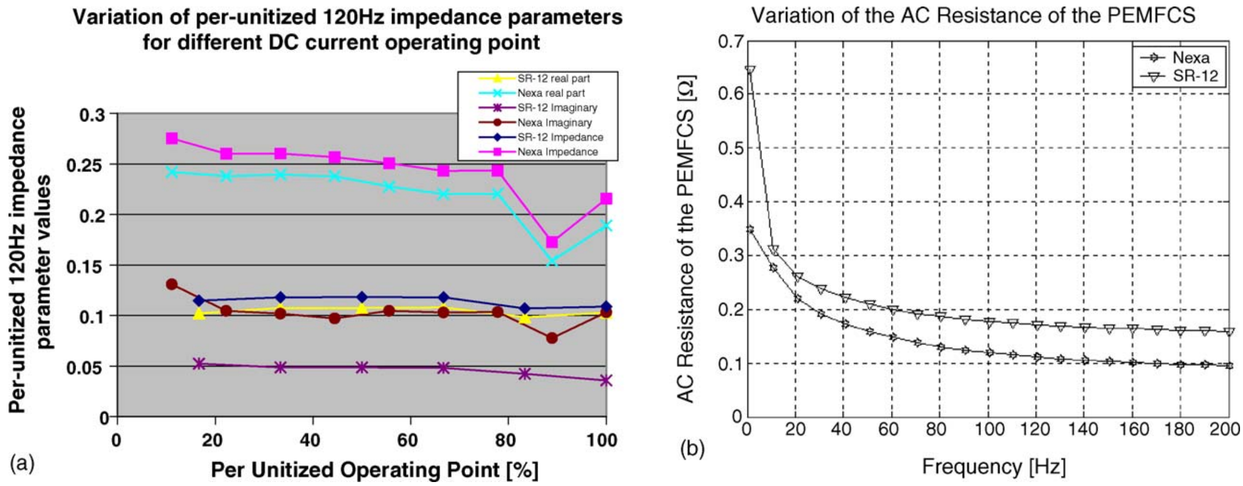

Fig. 10. (a) Variation of 120 Hz impedance parameters for different DC current loading conditions and (b) variation of the AC resistance of the PEMFCS at the rated condition.

It can be shown from (1)–(3) that,

$$\mathrm{VRF} = R_{\mathrm{P,\,per\text{-}unit}} \tag{4}$$

$R_{\mathrm{P,\,per\text{-}unit}}$ and VRF for each fuel cell stack can be calculated from Table 1. A fuel cell stack, which has a lower $R_{\mathrm{P,\,per\text{-}unit}}$ and VRF is considered to be better from the electrical performance point of view, since the variation in output voltage from no-load to full-load is minimal. Since a PCU is connected to the fuel cell output terminals, a larger VRF (variation in fuel cell output voltage) results in a larger volt-amp (VA) rating of the PCU. The VA rating of the PCU can be calculated as:

$$\mathrm{VA} = V_{\mathrm{o,\,no\text{-}load}} \times I_{\mathrm{full\text{-}load}} \tag{5}$$

Expressing (5) in per-unit, we have:

$$\mathrm{VA}_{\mathrm{per\text{-}unit}} = \frac{V_{\mathrm{o,\,no\text{-}load}} \times I_{\mathrm{full\text{-}load}}}{V_{\mathrm{base}} \times I_{\mathrm{base}}} \tag{6}$$

It can be shown from (1), (3) and (6) that,

$$\mathrm{VA}_{\mathrm{per\text{-}unit}} = \mathrm{VRF} + 1 \tag{7}$$

From (7) it is clear that a higher value of VRF results in higher rating (VA) of the power conditioning unit. Table 2 shows the corresponding VA ratings of the PCU for the fuel cells tested. A lower VA rating of the PCU is indicative of: the higher power semiconductor switching device and passive *L*–*C* component utilization (within the PCU) and the lower cost of the PCU.

2.2. AC equivalent circuit [6,7]

The objective of this test is to obtain the AC impedance of the fuel cell stack from zero to 10 kHz frequency. In this test (Fig. 2), the fuel cell is operated at a certain DC operating point on the *V*–*I* curve, and a small magnitude of sinusoidal AC current is superimposed. The current and corresponding voltage at the fuel cell terminals are recorded. From this data, the AC impedance of the fuel cell was computed. The above test is repeated from zero to 10 kHz frequency and the frequency response of fuel cell internal impedance was computed. Fig. 5 shows the magnitude and phase plot of the SR-12 fuel cell stack internal impedance variation from 0 to 10 kHz (for a DC current of 18 A, when perturbed by a sinusoidal AC current of 1 A in magnitude). The above impedance test is repeated at different operating points on the fuel cell *V*–*I* curve. Fig. 6(a and b) shows the Nyquist impedance plot of the computed impedance variation for SR-12 and Nexa PEMFCS respectively. From Fig. 6(a and b) it can be seen that the AC impedance variation of SR-12 is smaller than that of Ballard-Nexa fuel cell. The smaller variation in AC impedance for SR-12 (in Fig. 6a) can be attributed to its lower VRF value (see Table 2).

With the above measured impedance data, an electrical equivalent circuit of the fuel cell internal impedance is obtained as

Table 2
VRF and VA ratings of the PCU for the PEMFCs under test

Fuel cell type	$R_{\mathrm{P,\,per\text{-}unit}}$ (or VRF) see Eqs. (1)–(3)	VA ratings of the PCU in per-unit
SR-12	0.4 (or 40 [%])	1.4 (or 140 [%])
Nexa	0.586 (or 58.6 [%])	1.586 (or 158.6 [%])

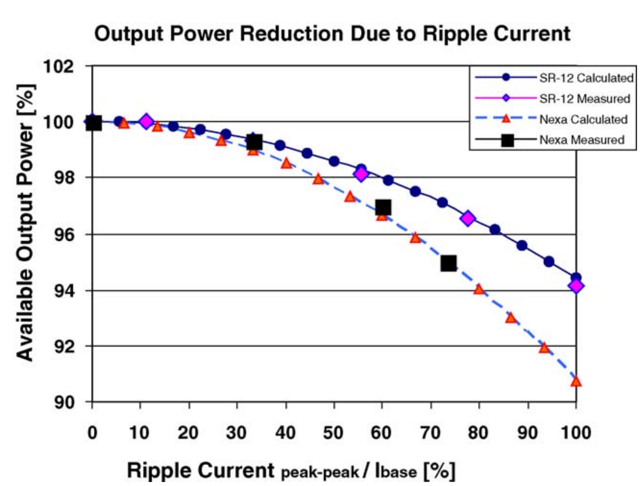

Fig. 11. Relationship between output power reduction and ripple current at the rated condition.

Table 3
Parameters of the electric equivalent circuit for the PEMFCs under test

Fuel cell type	R_1 [Ω]	R_2 [Ω]	R_3 [Ω]	R_4 [Ω]	R_5 [Ω]	R_6 [mΩ]	C_1 [mF]	C_2 [mF]	C_3 [mF]	L_1 [μH]
SR12	0.41	0.0115	0.17	0.15	0.085	0.07	80	9	2.5	2
Nexa	0.15	0.0115	0.15	0.15	0.065	0.07	70	7.5	5.5	4.8

follows. Since one semicircle in the Nyquist impedance plot (Fig. 6) corresponds to a single time constant (*R*–*C*), closer observation of Fig. 6 shows the existence of three such time constants. Further, the diameter of each semicircle is a representative of the resistor value and the vertex corresponds to the characteristic frequency. Using the above-described approach and the curve fitting technique, an electric equivalent circuit of the fuel cell and its parameters at a certain operating point was obtained from the measured data and is shown in Fig. 7 and Table 3. The equivalent circuit consists of *R*–*C* branches obtained from parameter extraction. The fitted curve (see Fig. 5), which represents the frequency response (obtained from the equivalent circuit (Fig. 7)) shows close agreement with the measured frequency data. It is clear from Fig. 7 that for DC conditions (zero frequency) the equivalent circuit parameters match the steady-state *V*–*I* data shown in Fig. 3.

3. Evaluation of the effect of inverter ripple current

An important variable in the design of the power conditioning unit for a fuel cell is the amount of ripple current that can be drawn from a fuel cell without causing any adverse affect. Since the reactant utilization is known to impact the mechanical nature of a fuel cell, it is suggested in [5] that the varying reactant conditions surrounding the cell (due to ripple current) govern, at least in part, the life time of the

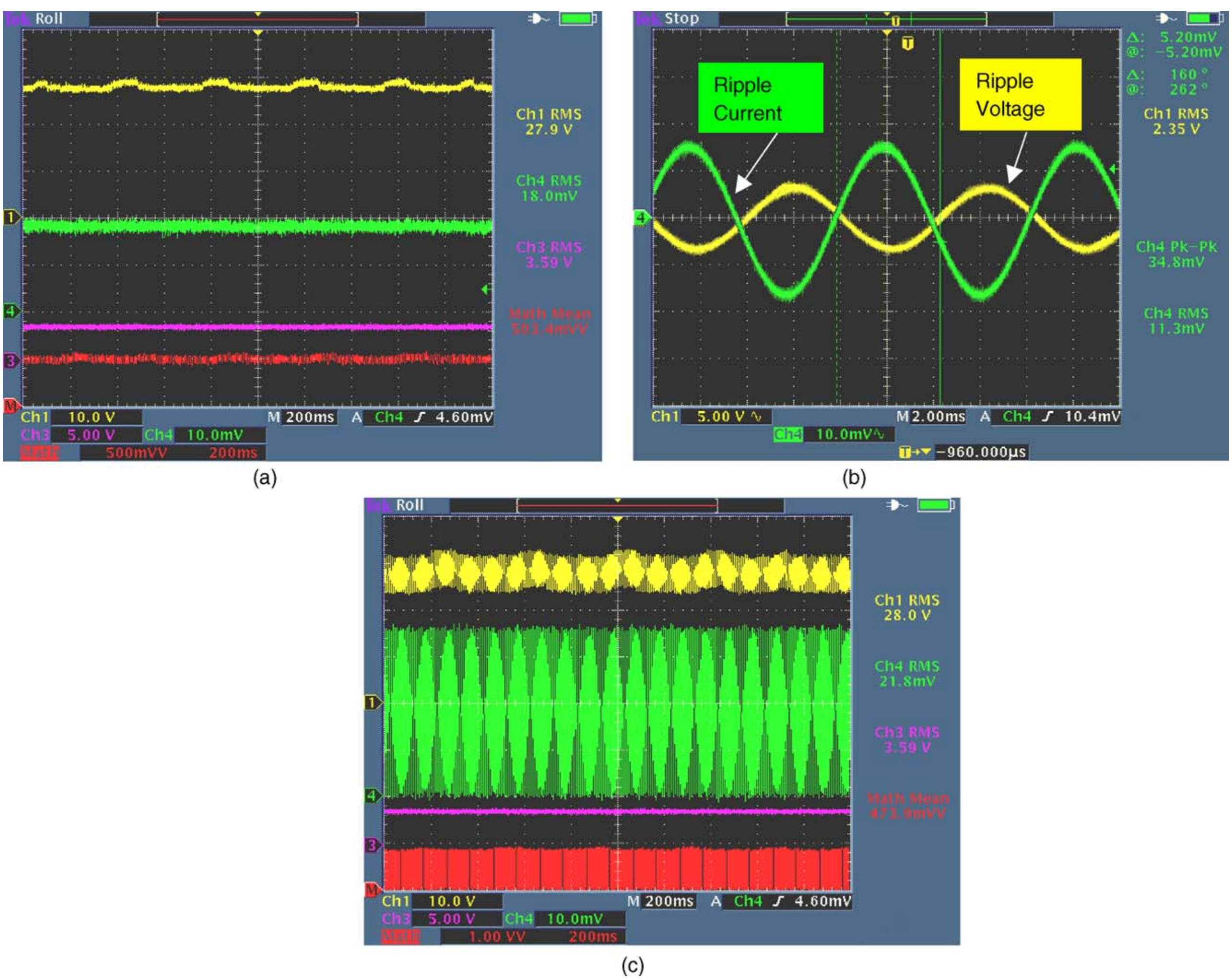

Fig. 12. (a) SR-12 loaded by a constant load (18 [A]), Channel-1: PEMFCS voltage [10 V div^{-1}], Channel-4: PEMFCS current [10 A div^{-1}], Channel-3: hydrogen flow rate [10 SLM div^{-1}], Channel-M: PEMFCS, output power [500 W div^{-1}], P_o = 503.4 [W], (b) SR-12 fuel cell terminal voltage and the ripple current for: 120 Hz ripple current (17.3 [A], peak-to-peak value) at the DC operating point of 18 [A], P_o = 473.9 [W], Hydrogen flow rate: 7.18 [SLM min^{-1}], (c) SR-12 loaded by a constant load (18 [A]) and a 120 Hz ripple (18 [A] peak-to-peak). Channel-1: PEMFCS voltage [10 V div^{-1}], Channel-4: PEMFCS current [10 A div^{-1}], Channel-3: hydrogen flow rate [10 SLM div^{-1}], Channel-M: PEMFCS output power, [1 kW div^{-1}], P_o = 473.9 [W].

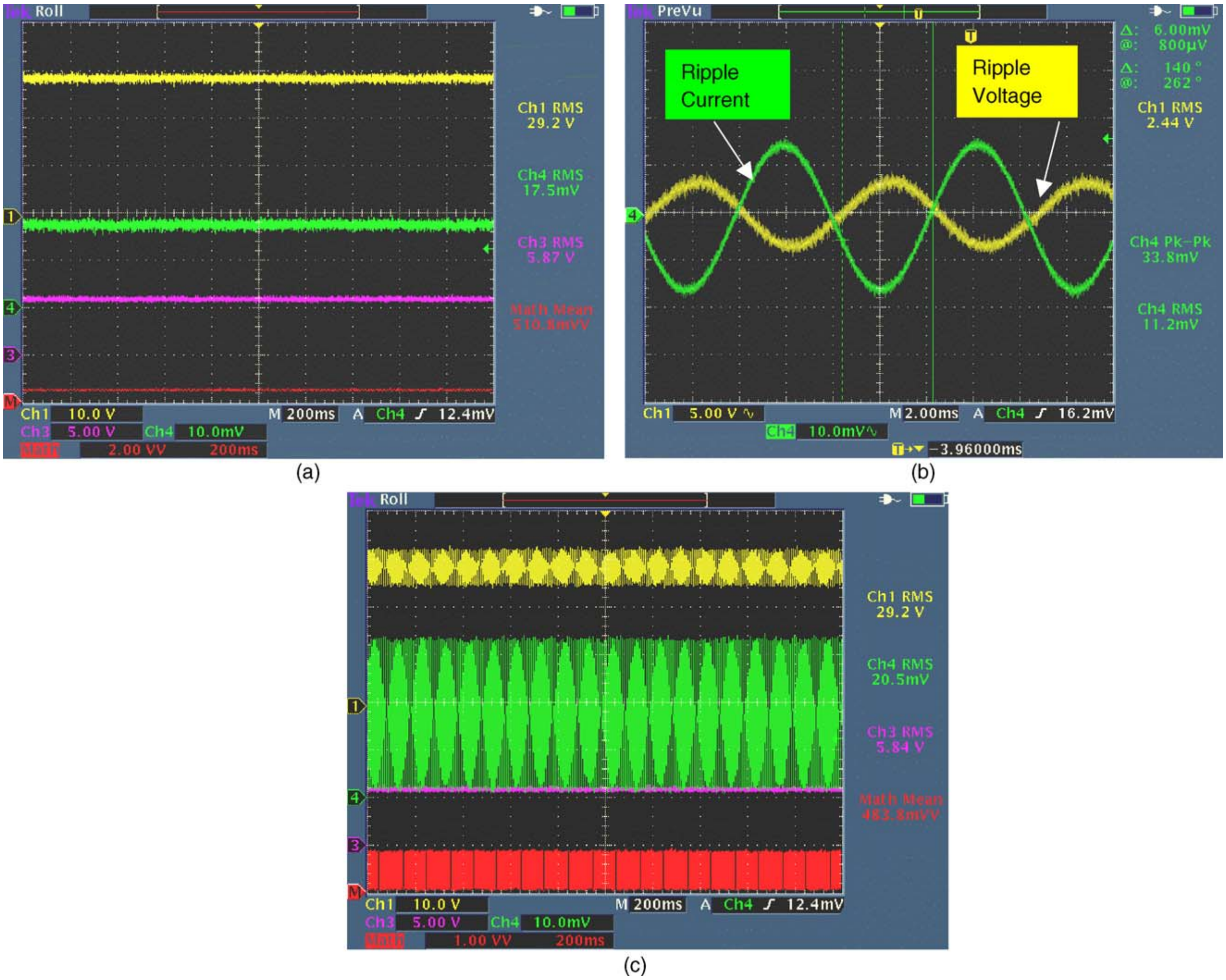

Fig. 13. (a) Nexa loaded by a constant load (35 [A]). Channel-1: PEMFCS voltage [10 V div^{-1}], Channel-4: PEMFCS current [20 A div^{-1}], Channel-3: hydrogen flow rate [10 SLM div^{-1}], Channel-M: PEMFCS, output power [2 kW div^{-1}], P_o = 1021.6 [W], (b) Nexa fuel cell terminal voltage and the ripple current for: 120 Hz ripple current (30.2 [A], peak-to-peak value) at the DC operating point of 35 [A], P_o = 967.6 [W], Hydrogen flow rate: 11.74 [SLM min^{-1}], (c) Nexa loaded by a constant load (35 [A]) and a 120 Hz ripple (30.2 [A] peak-to-peak), Channel-1: PEMFCS voltage [10 V div^{-1}], Channel-4: PEMFCS current [20 A div^{-1}], Channel-3: hydrogen flow rate [10 SLM div^{-1}], Channel-M: PEMFCS output power, [2 kW div^{-1}], P_o = 967.6 [W].

cells. Both the magnitude and frequency of the ripple current is important.

For fuel cells powering single-phase loads (60 Hz), the ripple current of concern is twice the output frequency, i.e. 120 Hz [8]. Ballard Nexa specifications indicate a limit of 24.7% rms (35% peak–peak) for 120 Hz ripple current [9]. It should be noted that switching frequency (20–60 kHz) components in the DC–DC converter are easily filtered via a small high frequency capacitive filter.

Fig. 8 shows the interconnection of the fuel cell equivalent circuit with the PCU. The PCU may be composed of any combination of switch-mode DC–DC converters, DC–AC inverters, filters and isolation transformers depending on the topology adopted. Fig. 9 and Table 4 show the AC equivalent circuit and its parameters of the fuel cell at 120 Hz frequency. This figure is obtained by setting $f = 120$ Hz in Fig. 7.

From Fig. 9 and Table 4, the impedance of the fuel cell stack at 120 Hz at the rated operating condition is:

$$\begin{aligned} Z_{120\,\mathrm{Hz}} &= 0.1717 - j0.06 = 0.1818\angle -19.26^\circ \quad (\mathrm{SR}-12) \\ &= 0.1115 - j0.061 = 0.1271\angle -28.68^\circ \quad (\mathrm{Nexa}) \end{aligned} \tag{8}$$

Table 4
Parameters of the AC equivalent circuit of the PEMFCs at 120 Hz frequency

Fuel cell type	$R_{120\,\mathrm{Hz}}$ [Ω]	$X_{C\_120\,\mathrm{Hz}}$ [Ω]	$R_{120\,\mathrm{Hz\_PU}}$	$X_{C\_120\,\mathrm{Hz\_PU}}$
SR-12	0.1717	0.06	0.1028	0.0359
Nexa	0.1115	0.061	0.1889	0.1034

Table 5
Summary of the measured values from the experiments

Fuel cell type	Output voltage [V_rms]		Output current [A_rms]		Output power [W]		H2 flow rate [SLM]	
	A	B	A	B	A	B	A	B
SR-12	27.9	28	18	21.8	503.4	473.9	7.18	7.18
Nexa	29.2	29.2	35	41	1021.6	967.6	11.74	11.68

A: Figs. 12a and 13a; B: Figs. 12c and 13c.

From the per-unit quantities defined in (1) we have,

$$Z_{120\,\text{Hz, per-unit}} = \frac{Z_{120\,\text{Hz}}}{Z_{\text{base}}} = R_{120\,\text{Hz, per-unit}} - \text{j}X_{120\,\text{Hz, per-unit}} = 0.1028 - \text{j}0.0359 = 0.1089\angle -19.26^\circ \quad \text{(SR-12)} = 0.1889 - \text{j}0.1034 = 0.2153\angle -28.69^\circ \quad \text{(Nexa)} \tag{9}$$

From (9) and Fig. 9, it is clear that the 120 Hz ripple current drawn by the PCU contributes to a loss equal to $I_{\text{Ripple}}^2 \times R_{120\,\text{Hz}}$. This loss can be interpreted as a reduction in the available output power from the fuel cell. The per-unit reduction in fuel cell output power due to ripple current can be computed as:

$$P_{\text{Loss, per-unit}} = I_{\text{Ripple, per-unit}}^2 \times R_{\text{120Hz, per-unit}} \tag{10}$$

In addition to power reduction, the ripple current (120 Hz) also contributes to AC voltage ripple (120 Hz) at the fuel cell output terminals. The magnitude of the AC ripple voltage also can be computed from Fig. 9 as:

$$V_{\text{Ripple, per-unit}} = I_{\text{Ripple, per-unit}} \times Z_{120\,\text{Hz, per-unit}} \tag{11}$$

4. Experimental results and discussion

Several experiments were conducted on the PEMFCS setup (Fig. 2). Fig. 10a shows the 120 Hz impedance variation for different DC current loading conditions of the fuel cells. It is noted that the impedance of the PEMFCS is a minimum around the 90% loading condition. From the figure, it can be observed that SR-12 shows almost no variation of its 120 Hz resistance value over the 20–100% operating range, while the Nexa shows a variation of 37%. This implies that the power reduction due to ripple current is almost the same at every operating point in the case of SR-12, however it becomes severe in the lower range of the operation in the case of Nexa.

Fig. 11 shows the variation of fuel cell available power (at the rated condition) as a function of ripple current as predicted by Eq. (10) and the measured results. It is noted that in the extreme case of 100% ripple (120 Hz), the available power is reduced by 5.86% in SR-12 and 9.4% in Nexa. Further, for 30% ripple, the reduction in output power from SR-12 is 0.5% and 0.84% from Nexa.

Figs. 12a and 13a show the terminal voltage, current, hydrogen input flow rate and fuel cell output power when the fuel cell is supplying a DC load. Figs. 12b and 13b show the fuel cell terminal voltage distortion when supplying a ripple current of 120 Hz superimposed on the DC current. Figs. 12c and 13c confirm the power reduction due to the ripple current with no change in the hydrogen input flow rate. Therefore, it is clear from this fact that if the 120 Hz ripple currents exist at the output of the fuel cell stack, more fuel is required to get a certain amount of power. All the measured values from the experiments are summarized in the Table 5.

5. Conclusion

In this paper an impedance model of the PEMFCS has been developed from experiments. Experimental results show that the developed model explains the electrical characteristics of the fuel cells when connected to a power conditioning unit (PCU). The relationship between the fuel cell output voltage variation and the volt-amp rating of the PCU has been shown. It has been shown experimentally that PCU ripple current (120 Hz) can contribute to a reduction in the fuel cell available output power and increased distortion of the terminal voltage. Limiting the low frequency (120 Hz) fuel cell ripple current to between 30% and 40% has been shown to result in less than 0.5–1.5% reduction in fuel cell output power, and therefore, may be acceptable. Restricting the ripple current below these values will require a more robust input *L–C* filter within the PCU. Additional losses within the PCU's *L–C* filter then become a concern and contribute to a lower PCU efficiency. The results presented in this paper can be used to further optimize the overall efficiency and cost of a fuel cell and its PCU. These results will be presented in a companion paper in the near future.

Acknowledgement

This work was supported by the Soongsil University Research Fund.

Appendix A. Specification of PEM fuel cell stack

	SR-12	Nexa
Rated power	500 W	1200 W
Output voltage	25–39 VDC	22–50 VDC
Fuel purity (minimum)	99.95 [%] H2	99.99 [%] H2
Fuel consumption	7.0 SLPM at 500 W	18.5 SLPM at 1200 W
Start-up time (cold start)	7 min	2 min
Operating temperature	5–35 °C	3–40 °C
Number of cells	48	48

References

[1] G. Maggio, V. Recupero, L. pino, Modeling polymer electrolyte fuel cells: an innovative approach, J. Power Source 101 (2001) 257–286.

[2] J.C. Amphlett, R.F. Mann, B.A. Peppley, P.R. Roberge, A. Rodrigues, A model predicting transient responses of proton exchange membrane fuel cells, J. Power Source 61 (1996) 183–188.

[3] M.D. Lukas, K.Y. Lee, H. Ghezel-Ayagh, An explicit model for direct reforming carbonate fuel cell stack, IEEE Trans. Energy Convers. 16 (3) (2001) 289–295.

[4] J.M. Correa, F.A. Farret, L.N. Canha, An Analysis of the Dynamic Performance of Proton Exchange Membrane Fuel Cells Using an Electrochemical Model, In: The 27th Annual Conference of the IEEE IECON, vol. 1, 2001, pp. 141–146.

[5] R.S. Gemmen, Analysis for the effect of the ripple current on fuel cell operating condition, ASME 369 (4) (2001) 279–289.

[6] J.R. Macdonald, Impedance Spectroscopy: Emphasizing Solid Materials and Systems, John Wiley & Sons, Inc., 1987.

[7] J.R. Sleman, Y.P. Lin, Application of AC impedance in fuel cell research and development, Electrochem. Acta 38 (14) (1993) 2063–2073.

[8] P. Enjeti, Power Conditioning Systems for Fuel Cell Systems, sixth ed., US Department of Energy Fuel Cell Handbook, 2002 (Chapter #9).

[9] Ballard Nexa® Power Module User's manual.